

## Numerical and experimental diagnostics of rf discharges in pure and dusty argon

Ph. Belenguer

*Centre de Physique Atomique de Toulouse, Université Paul Sabatier, 118 route de Narbonne, 31062 Toulouse CEDEX, France*

J. Ph. Blondeau, L. Boufendi, M. Toogood, A. Plain, A. Bouchoule, and C. Laure

*Groupe de Recherche sur l'Energétique des Milieux Ionisés, UFR Sciences—Université d'Orléans, Boîte Postale 6759, 45067 Orléans CEDEX 02, France*

J. P. Boeuf

*Centre de Physique Atomique de Toulouse, Université Paul Sabatier, 118 route de Narbonne, 31062 Toulouse CEDEX, France*

(Received 10 June 1992)

Self-consistent fluid and particle-in-cell Monte Carlo (PIC-MC) models in conjunction with experimental measurements have been used to study the electrical characteristics of rf discharges in pure argon and in argon contaminated with dust particles (at 0.11 torr argon, 13.56 MHz). In the experiments, the dust particles were first created in a silane-argon rf discharge and subsequently trapped in an argon discharge in order to stop the growth process. The concentration and radius of the dust particles were measured experimentally and found equal to  $10^8 \text{ cm}^{-3}$  and  $0.05 \text{ }\mu\text{m}$ , respectively. The PIC-MC discharge model has been used to check the validity of the fluid model in pure argon. The discharge in dusty argon has been described with a fluid model modified to account for the presence of dust particles. This model uses as input data the number of negative charges carried by the dust particles and the frequency of electron loss to the particles deduced from a two-dimensional particle-in-cell Monte Carlo simulation of a dusty dc plasma. The results show good agreement between experiments and models within the whole range of rf voltages considered and for the pure and dusty argon plasmas. The presence of dust particles in the plasma modifies considerably the discharge impedance, which becomes much more resistive. The electron number density in the plasma is much smaller than the positive ion density and than the number density of negative charges carried by the dust particles. It appears that the phase shift between current and voltage is very sensitive to the presence of powders. This property could be useful for the detection of powder formation in a processing plasma.

PACS number(s): 52.80.Pi, 52.25.Fi

### I. INTRODUCTION

The appearance of dust particles in low-pressure plasmas used in material processing for sputtering, etching, or deposition is now recognized as an important factor of device-yield-reducing contamination for the semiconductor manufacturing industry. Selwyn, Singh, and Bennet have reported [1] that 50% of device yield loss can be attributed to particle contamination. However, a positive aspect of particle formation in plasmas is the fabrication of nanoscale particles for material applications [2]. Anderson, Jairath, and Mock [2] have fabricated silicon-nitride particles in a low-pressure discharge in a  $\text{SiH}_4/\text{NH}_3$  mixture.

Particle formation in low-pressure plasmas and the study of the perturbations induced by these particles on the plasma properties have recently attracted the interest of modelers [3–7]. Dust particles immersed in a weakly ionized plasma behave as electrostatic probes and acquire a negative charge and a floating potential negative with respect to the plasma potential. The role of the floating potential is to repel electrons which are much more mobile than ions and to attract positive ions to ensure an exact balance between the electron and the ion fluxes to the dust particles at steady state. In order to compensate for the loss of electrons and ions to the dust particles, the

plasma electric field must increase so as to increase the production of charged particles by ionization. The electron-energy distribution function in the plasma column is modified in the presence of powders with respect to the pristine case not only because the electrons with an energy larger than the floating potential of the particles can be absorbed by the particles, but also, and more importantly, because the plasma electric field must be much higher in a dusty plasma.

Dramatic changes in the electrical characteristics of the plasma have been observed due to the presence of particles. It is the goal of this paper to provide a better understanding of these changes and a better insight into the physics of a dusty plasma by comparing experimental measurements with results of self-consistent numerical modes in pure and dusty discharges. A spectacular example of these changes in the plasma impedance is given in Ref. [8] where a sharp transition from a capacitive to a resistive behavior was observed above a critical applied voltage in a rf discharge in pure silane. With the help of numerical models of the discharge, this transition was attributed to the formation of dust particles [9]. In the present paper and in order to make possible direct and simple comparisons between experiments and models, the conditions of the experiments were chosen in such a way that the concentration and size of the dust particles were

controlled and kept constant during the measurements. The particles were created in a silane-argon rf discharge and subsequently trapped in a rf discharge in pure argon. The silane being removed, the growth processes of the dust particles were therefore stopped and it was possible to measure the electrical characteristics of an argon plasma contaminated with powders of known density and size. The concentration and size of the dust particles were measured using the experimental techniques described in previous papers [10,11], namely, Mie laser light scattering and transmission electron microscopy (dust particle concentration  $10^8 \text{ cm}^{-3}$  and particle radius  $0.05 \mu\text{m}$ ). Electrical characteristics of both pure and contaminated argon plasmas measured experimentally and calculated theoretically have been compared under the same conditions of pressure, geometry, and frequency. The models are based on a self-consistent description of the charged-particle transport and electric field. Two important parameters are necessary in order to account for the presence of dust particles in the models: (1) the number of negative charges carried by the particles and (2) the electron loss frequency to the dust particles. These parameters were deduced from a 2D particle-in-cell Monte Carlo (PIC-MC) simulation of a uniform, dusty dc plasma (see related paper, Ref. [7]) for conditions of particle concentration and size identical to those of the experiment.

The experimental setup and the principles of the experiments are described in Sec. II. Section III presents an overview of the physical basis of the model. Experimental and numerical results are discussed in Sec. IV which includes comparisons between results from fluid and particle models and experiments in pure argon as well as comparisons between results from the fluid models and experiments in a dusty argon discharge. A few concluding remarks are given in Sec. V.

## II. MEASUREMENTS

### A. Experimental setup

Experiments were carried out in a confined parallel-plate rf chamber as has been described previously in detail [10]. The upper rf powered electrode is a stainless-steel grid 13 cm in diameter and the lower grounded electrode is a stainless-steel cylindrical box 13.5 cm in diameter with a grided bottom for laminar gas flow. The distance between electrodes is 3.3 cm. The discharge configuration is not perfectly symmetric, but the self-bias voltage was small with respect to the rf voltage in all the results described below. The rf voltage  $V(t)$  is measured by a capacitive divider when the current-voltage phase shift is required and a Tektronix P6015 probe when the self-bias voltage is required. In order to obtain the effective current in the discharge we have used a capacitive current subtraction system which is illustrated in Fig. 1 and has been described in detail elsewhere [10].

The rf current which flows through the reactor contains two components: a large one,  $I_c(t)$ , due to the stray capacitance of the discharge box (100 pF), and the much smaller rf current  $I_p(t)$ . The system we have developed

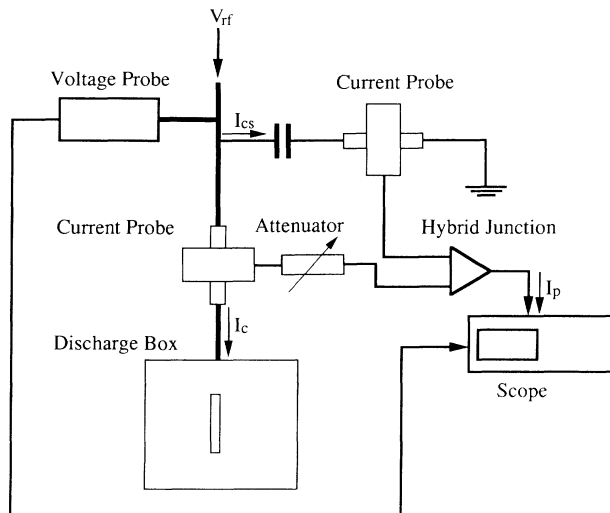


FIG. 1. Experimental setup.

allows the stray capacitive current to be eliminated by subtraction. An additional capacitor (20 pF) gives a subsidiary capacitive current excited by the same voltage. Two identical homemade current probes (50 MHz bandwidth) sense these two currents which are subtracted through a wide band hybrid junction. The capacitive currents are adjusted with precision attenuators until they cancel, by making measurements in the absence of plasma. The net current obtained with the discharge on is therefore the rf current  $I_p(t)$ . The probe signals  $I_p(t)$  and  $V_{rf}(t)$  are measured on the two channels of a Tektronix 2440 (500 MHz) digital oscilloscope and stored on a PC 386 with an IEEE interface. The amplitude of  $I_p(t)$  and  $V_{rf}(t)$  as well as their phase shift are deduced from these measurements. It was observed that  $I_p(t)$  for a pure argon plasma is not perfectly sinusoidal but becomes more so when dust particles are present. Therefore the wave forms were analyzed either by Fourier transform or by using a 20-MHz bandpass filter on the oscilloscope input in order to measure the phase shift  $\phi$  and calculate the effective power dissipated

$$P = \frac{1}{2} I_p V_{rf} \cos(\phi)$$

by taking into account only the fundamental harmonic [8].

### B. Experimental procedure

It is known that negatively charged heavy particles are trapped in a rf discharge [10,12] and a method was developed to first produce dust particles of known size and concentration in a rf discharge in argon containing a few percent of silane and then confine them in a rf discharge in pure argon. The argon-silane discharge was run typically for 5 s to allow for the formation of (silicon-based) dust particles whose size distribution was close to being monodisperse [11]. The silane flow was then cut in order to stop the growth process of the particles. Measurements of the electrical characteristics of the

remaining dusty argon plasma were then performed when a steady-state regime was reached. To recreate a pure argon plasma and perform similar measurements for comparisons, the plasma was extinguished for about 2 s; this time was sufficient to remove the dust particles (no longer trapped by the electric field) from the chamber. The electrical characteristics were thus obtained for a variety of rf voltages (75–300 V) while keeping all other conditions constant: total pressure, 117 mtorr; argon flow, 30 sccm; silane flow during 5 s, 1.2 sccm.

It has been checked by light scattering measurements that the dust particles concentration remains approximately constant (less than a few percent decrease) during the time necessary to measure the electrical characteristics of the discharge. On the other hand, the experiments show that under the conditions considered, the axial profile of the dust particle concentration does not exhibit large peaks at the plasma-sheath boundary as has been observed in other conditions and is roughly spatially constant in the plasma.

### III. PHYSICAL AND NUMERICAL MODELS

Self-consistent electrical models have been used to calculate the current versus voltage characteristics and other properties of the rf discharge in pure argon and in contaminated argon. Results from the models and comparisons with experiments are described in Sec. IV.

The physical models are based on a description of electron and ion transport coupled with Poisson's equation. Fluid and particle models of the plasma have been used in the case of pure argon. In the case of argon contaminated with dust particles, a fluid model has been used to represent electron and ion transport. The size and concentration of dust particles are assumed to be constant and their values are taken from the experiment. The influence of negatively charged dust particles on the plasma is taken into account in the model as described in Sec. III B. We briefly describe below the fluid and particle models.

#### A. Fluid and particle models

An electrical model of the discharge and of its associated plasma consists of a description of the coupling between the charged-particle transport phenomena and the electric field. In this paper we use two different approaches to describe the charged-particle transport, (a) a fluid or macroscopic description of the properties of the charged particles and (b), a particle or microscopic approach. Fluid models have been useful to better understand the basic mechanisms of radio-frequency discharges [13–18] and have proved to be sufficiently accurate under many conditions to predict quantitatively the electrical behavior of the discharge. In fluid models the charged-particle properties are characterized by macroscopic quantities such as density, mean velocity, and mean energy which are solutions of the first three moments in velocity space of the Boltzmann equation. The main difficulty in closing the system of moment equations in the context of an electric discharge is in the estimation of

the ionization rate. In this paper we have used a two-electron-group fluid model of the discharge similar to one presented in Refs. [17,18]. Each electron group is described by two moment equations. The bulk electrons are described with continuity and momentum (drift-diffusion approximation) equations, assuming local equilibrium between the field and the bulk electron distribution function. A second group consists of those electrons emitted by the electrodes and accelerated through the sheaths. This second group is described by continuity and energy equations assuming a monoenergetic electron distribution. The ions are treated as one group in the same manner as the bulk electrons. The data used in the fluid model for bulk electrons and ions are transport coefficients (drift velocity, diffusion coefficient, and ionization coefficients). Mobility and the ionization coefficient as a function of the reduced electric field  $E/p$  ( $E$  is the electric field,  $p$  the pressure) have been taken from Ward [19]. Diffusion coefficients are supposed to be constant and equal to  $3 \times 10^5 \text{ cm}^2 \text{ s}^{-1}$  for electrons and to  $2 \times 10^2 \text{ cm}^2 \text{ s}^{-1}$  for ions (at 1 torr, ambient temperature). The electron-neutral cross sections used in the energy equation of the second group of electrons are the same as those used in the PIC-MC model described below.

Fluid models become less accurate in the low-pressure regime which is less collisional and the local equilibrium assumption for the bulk electrons fails. Since the experiments have been done at relatively low pressure (110 mtorr) the validity of the fluid model must be assessed. We have therefore also used a much more accurate approach based on particle-in-cell Monte Carlo techniques in order to confirm the validity of the fluid model in these conditions.

The PIC-MC model is based on a microscopic description of the electron and ion transport and is identical to the one used in Ref. [9]. The trajectories of a sample of particles, electrons, and ions are followed in velocity-position space. The equations of motion are integrated between collisions in a given electric field, and the field is recalculated using a particle-in-cell method [20] at short time intervals. Collisions (time, nature, and scattering angle) are determined on the basis of random numbers generated according to probability density laws related to the charged-particle-neutral cross section, as in Monte Carlo simulations [21]. Similar PIC-MC techniques have been described by Boswell and Morey [22], Surendra and Graves [23], and Birdsall [24]. In the results presented below, more than 1000 cycles were followed, the number of simulated charged particles of each kind being of the order of 15 000. The basic data needed in a PIC-MC model are electron and ion-neutral collision cross sections. The electron atom cross sections are taken from Ref. [25]. Concerning the ion-atom collisions, only charge exchange has been considered, with a constant cross section of  $2 \times 10^{-15} \text{ cm}^2$ .

As mentioned above, fluid models can be inaccurate due to the inherent assumptions of the charged-particle velocity distribution functions. PIC-MC models are in principle more accurate because such assumptions are not needed, the distribution functions being calculated in a self-consistent way. However, inaccuracy can occur in

PIC-MC models due to numerical heating. In order to avoid numerical errors, parameters such as the number of simulated particles, number of simulated rf cycles, the grid spacing, and the integration time step must be chosen carefully according to the Debye length and plasma frequency of the problem. It is difficult to estimate the numerical error to be expected for a given set of these parameters and more work is needed to study this question.

### B. Model of a dusty rf discharge

As described in Sec. IV below, the comparisons of the fluid and particle models in pure argon show that the fluid approach is reasonably accurate for the conditions of the experiments (0.11 torr). Thus, only the fluid model has been used for the simulation of an rf discharge in dusty argon.

Dust particles in a weakly ionized plasma behave as electrostatic probes. Due to the large mobility of electrons compared with that of ions, the dust particles acquire a negative charge and a floating potential which is negative with respect to the plasma potential. The floating potential repels electrons and attracts ions and adjusts in such a way that at steady state, the flux of electrons to the dust particle is exactly compensated by the ion flux. The loss of charged particles on the dust particles must be balanced by more ionization in the volume and the average electric field in the plasma must increase to satisfy this balance (just as in a positive column plasma surrounded by walls, where the average electric field is directly related to the electron and ion loss to the walls [26]). For large concentrations of dust particles such as in our experiment ( $10^8 \text{ cm}^{-3}$ ), the distance between dust particles (of the order of  $20 \mu\text{m}$ ) can be much smaller than the electron Debye length. Under such conditions, the electrons and positive ions cannot shield the charge of a dust particle within a distance smaller than the distance between particles. The two-dimensional (2D) PIC-MC model of a dusty plasma described in the companion paper [7] has shown that in the conditions of our experiments, the electron density should be much smaller than the positive-ion density. The dominant charge species in the plasma are therefore positive ions and negatively charged dust particles. The number of charges and the floating potential of dust particles as well as the frequency of electron and ion loss to the particles has been deduced from the simulation in Ref. [7], for conditions similar to our experimental conditions here. The aim of the model described below is, using results from the 2D PIC-MC model of a dusty plasma, to deduce self-consistently the electrical properties (current-voltage characteristics, etc.) of a rf discharge in contaminated argon and to compare these results with experiments. Good agreement between calculations and experiments would confirm some of the predictions of the 2D PIC-MC model.

The presence of powders in the plasma has been taken into account in the fluid model as follows. From the experimental measurements the size and concentration of dust particles are known. Further, the experiments show

that under the conditions considered, the dust particle concentration within the plasma is roughly spatially constant (the powders do not accumulate at the plasma sheath boundary as has been observed in other conditions). The 2D PIC-MC simulation [7] mentioned above has provided the floating potential and number of negative charges carried on the average by each dust particle. From this calculation we also know the average electric field which must exist in the plasma in order that electron and ion lost by recombination on the particles be compensated by ionization. In addition, the simulation provides the electron distribution function and hence the average frequency of electron loss on the dust particles (which is exactly equal to the ionization frequency since no other electron losses are considered). On the basis of the knowledge of the dust particle density  $n_D$  (given by the experiment) and of the number of negative charges  $Z_D$  and electron loss frequency  $\nu_D$  (given by the 2D PIC-MC model of Ref. [7]), we can build a complete model of a rf discharge in contaminated argon. Although the simulations of Ref. [7] correspond to a dc dusty plasma, we expect these results to be still valid under rf conditions because the electron and ion densities in the plasma are not modulated at 13.56 MHz. The fact that the plasma field is modulated in a rf discharge should not change significantly the results of Ref. [7], as discussed in Sec. IV (for consistency, we must check that the rms plasma field deduced from the rf discharge model is close to the dc field necessary to sustain the plasma predicted by the simulations of Ref. [7]). Note that the only force acting on powders which has been taken into account is the force due to the electric field. Other effects such as ion drag are neglected. This approximation seems reasonable in our conditions, since no accumulation of dust particles at the sheath-plasma boundary has been observed in the experiments and the axial profile of the dust particle concentration was roughly constant.

The main changes introduced in the fluid model described above for pure argon, to account for the presence of dust particles, are as follows.

(1) The charge density ( $Z_D n_D$ ) of dust particles is taken into account in Poisson's equation. In the conditions of the experiments which are simulated here, the value of  $Z_D$  deduced from the 2D PIC-MC model of a dusty argon plasma is on the order of 30 for current densities in the mA/cm<sup>2</sup> range.

(2) The profile of the distribution of dust particles in the plasma is obtained by assuming that they behave as heavy negative ions and by solving a continuity equation (drift-diffusion form) with no source term. The value of the dust particle density in the plasma center is imposed and taken equal to the experimental value ( $10^8 \text{ cm}^{-3}$ ). The density of negative charges corresponding to dust particles in the plasma center is therefore  $3 \times 10^9$  elementary charges per cm<sup>3</sup> ( $Z_D n_D$ ).

(3) The electron and positive-ion source terms in the corresponding continuity equations are modified to include the electron and ion losses on the dust particles (the loss rates for electrons and ions are identical, i.e., the number of negative charges and the floating potential of dust particles are assumed to be constant in space and

time). These source terms can be written as

$$S(x,t) = S_i(x,t) - n_e(x,t)\nu_D,$$

where  $S$  is the total source term of the electron ion continuity equations at position  $x$  and time  $t$ ,  $S_i$  is the local ionization rate estimated as in pure argon,  $n_e$  is the electron density, and  $\nu_D$  is the electron loss frequency on the dust particles. Under the conditions of the experiments, (0.11-torr argon, dust particle concentration  $10^8 \text{ cm}^{-3}$ , and radius  $0.05 \text{ }\mu\text{m}$ ), the 2D PIC-MC model [7] gives  $\nu_D \sim 3 \times 10^6 \text{ s}^{-1}$ . (Results are presented in Ref. [7] for  $n_D = 10^8 \text{ cm}^{-3}$  and dust particle radii of 0.1, 0.2,  $0.3 \text{ }\mu\text{m}$  only. The value of  $\nu_D$  for a radius of  $0.05 \text{ }\mu\text{m}$  has been obtained with the same code as in Ref. [7].) Results will also be presented in Sec. IV for other values of  $\nu_D$  in order to determine the sensitivity of the discharge model to the value of this parameter.

Note finally that, as in Ref. [7], only direct electron impact ionization from the ground state has been taken into account (this approximation is discussed in Ref. [7]).

Apart from the above changes, the model is similar to the two-electron-group fluid model used for pure argon and described in details in Refs. [17,18].

To summarize, the input data related to the presence of dust in the plasma which are needed in the fluid model are (1) dust particle concentration and size given by the experiment and (2) number of negative charges per particle and electron loss frequency on the dust particles given by the 2D PIC-MC model. Knowing these data, the rest of the model is similar to a classical, self-consistent electrical model of rf discharges. Since  $Z_D$  and  $\nu_D$  are taken from an independent 2D PIC-MC simulation of a uniform dc dusty plasma described in Ref. [7], we must check *a posteriori* that the results obtained from the fluid model are consistent with other data deduced from the simulations of Ref. [7] (such as rms electric field in the plasma and positive ion to electron number density ratio). This point will be discussed in Sec. IV.

## IV. RESULTS

### A. Pure argon

The results presented in this section have been obtained for an argon pressure of 0.11 torr, a gap length of 3.3 cm, and a frequency of 13.56 MHz. The left electrode is grounded and the right electrode is at the potential  $V(d,t) = V_{\text{rf}} \cos(\omega t)$ . The amplitude  $V_{\text{rf}}$  of the applied voltage varies from 50 to 300 V. In the numerical calculations, the secondary emission coefficient  $\gamma$  due to ion bombardment of the electrodes was supposed to be 0.06. Comparisons between fluid, PIC-MC models, and experiments are shown below.

#### 1. Comparisons between fluid and PIC-MC models

Figure 2 shows the spatial variations of the electron and ion densities and electric field for a discharge in pure argon at  $V_{\text{rf}} = 200 \text{ V}$  at the phase where the right electrode is the anode ( $t=0$ ). Results from the fluid model (solid lines) and the PIC-MC model (symbols) are com-

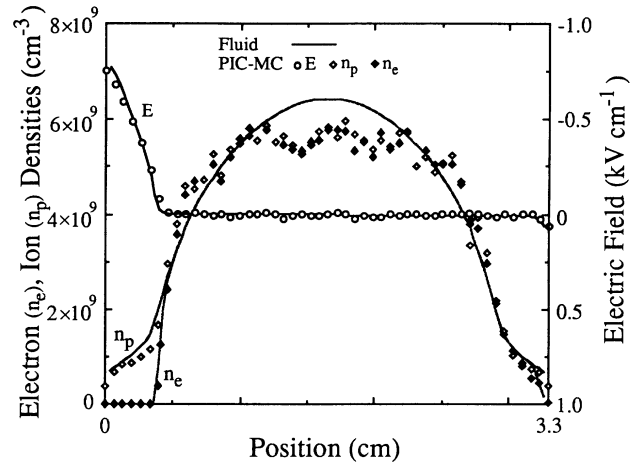


FIG. 2. Spatial variations of the charged particle number densities and electric field at the beginning of a rf cycle (the applied voltage is maximum on the right electrode) in pure argon (0.11 torr, 13.56 MHz) obtained with a fluid model (solid lines) and a PIC-MC simulation (symbols).

pared on this figure. The agreement between the fluid and PIC-MC models is surprisingly good for the relatively low pressure. Note, however, that the pressure under which a fluid model becomes inaccurate depends very much on the gas considered. In helium, for example, where the electron-atom cross sections are lower than for argon, higher pressures are needed for the fluid model to be valid. Figure 3 shows a comparison of the plasma density obtained with the fluid and PIC-MC models for different values of the applied voltage. The agreement between the two models appears to be good over the whole range of applied voltages considered. We mentioned in Sec. III A that fluid models and PIC-MC models can be inaccurate due to some inherent assumptions on the charged particle transport properties (fluid models) or to

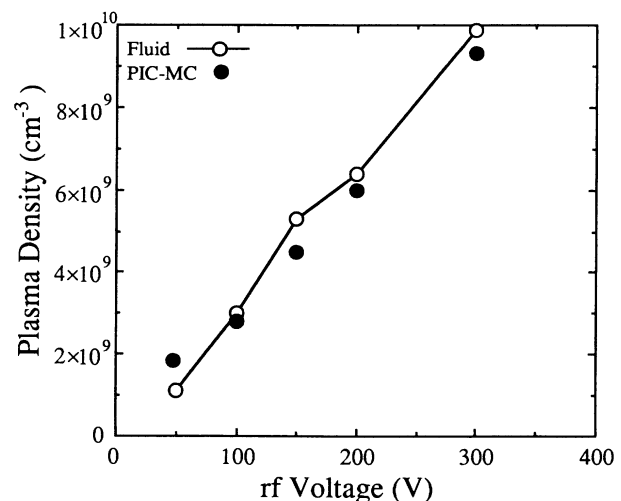


FIG. 3. Plasma density as a function of applied rf voltage from the fluid and PIC-MC models in pure argon; same conditions as in Fig. 2.

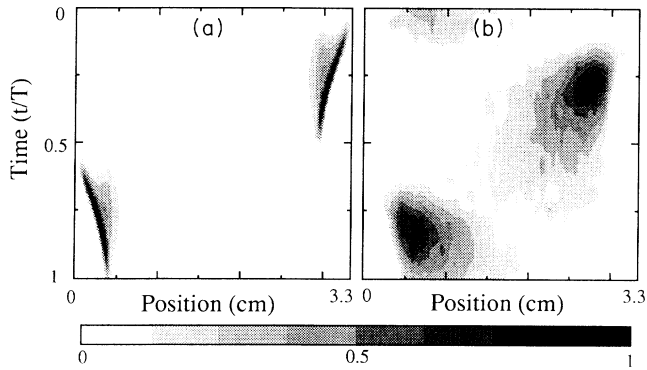


FIG. 4. Space and time variations of the ionization rate over one rf cycle in pure argon in the conditions of Fig. 2; (a) fluid model, unit =  $6.2 \times 10^{15} \text{ cm}^{-3} \text{ s}^{-1}$ ; (b) PIC-MC model, unit =  $1.7 \times 10^{15} \text{ cm}^{-3} \text{ s}^{-1}$ .

numerical heating (PIC-MC). Although it is difficult to estimate these errors, the fact that these very different approaches (fluid and particle models) lead to similar results over a relatively large range of applied voltages increases our confidence in the results.

As mentioned above, the main difficulty in a fluid model consists in describing accurately the ionization mechanisms in the discharge. It is then interesting to compare the ionization rates obtained by the fluid model and the PIC-MC model. Figure 4 represents the spatial and temporal variations of the ionization rate (source term in the electron and positive-ion continuity equations) obtained with each model for the same conditions as in Fig. 2. Larger ionization rates correspond to darker regions on the diagrams of Fig. 4, but note that the scale is different for the two models. Qualitatively the two models give similar results. For the frequency used in this work (13.56 MHz), ionization occurs mainly during the sheath expansion. This ionization mechanism, due to electrons accelerated by the sheath expansion (and termed as “wave riding”), has been described previously by different authors (see, e.g., Refs. [18,23]) and is typical of high-frequency discharges. The fluid model indicates that the contribution of the secondary electrons to the overall ionization is less than 20%, the dominant sustaining mechanism being therefore the sheath oscillations in these conditions. As could be expected from the local field assumption used for the bulk electrons in the fluid model, the ionization rate deduced from the fluid model is more localized than in the PIC-MC model. The more accurate PIC-MC model shows that bulk electrons accelerated during the sheath expansion actually release their energy a little bit deeper into the plasma than predicted by the fluid model. It is, however, interesting to note that although the spatial distributions of the ionization rate predicted by each model are not identical, the space and time-averaged ionization rates deduced from the fluid and PIC-MC models are in excellent agreement over the whole range of applied voltages considered (see Fig. 5). This is the reason the main macroscopic characteristics of the discharge predicted by both models are in good agreement.

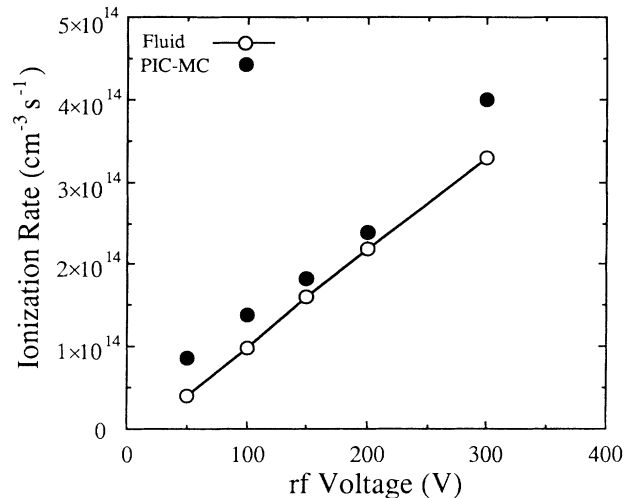


FIG. 5. Space and time-averaged ionization rate in pure argon as a function of applied rf voltage from the fluid and PIC-MC models; same conditions as in Fig. 2.

## 2. Comparisons between models and experiments

Figure 6 represents the variation of the total current density as a function of the applied voltage. The fluid (open circles) and PIC-MC (open triangles) models give almost identical results and reproduce the current obtained experimentally (solid circles). The current varies quite linearly from a fraction to a few  $\text{mA cm}^{-2}$ . The discrepancy between the numerical results and the experiments is less than a factor of 2 and is more important at higher applied voltages. These results indicate that the models are able to describe with a reasonable accuracy the electrical characteristics of the discharge under these conditions. Figure 7 shows the variations of the cosine of the current-voltage phase shift for the same conditions as Fig. 6. The discharge has a capacitive behavior at large

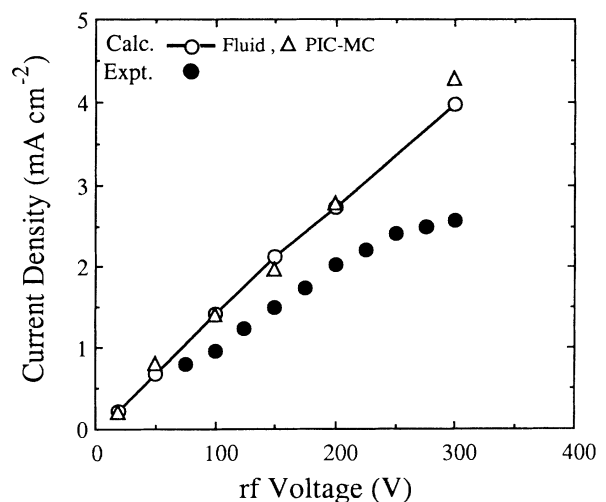


FIG. 6. Current density in a rf discharge in pure argon as a function of applied rf voltage from experiments and fluid and PIC-MC models; same conditions as in Fig. 2.

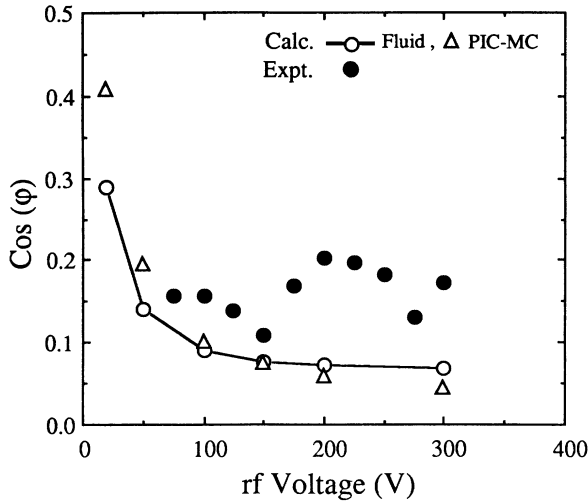


FIG. 7. Cosine of the current-voltage phase shift,  $\cos(\varphi)$ , in a rf discharge in pure argon as a function of applied rf voltage from experiments and fluid and PIC-MC models; same conditions as in Fig. 2.

rf voltages, the phase shift between current and voltage being close to  $\pi/2$ . The models indicate that the discharge becomes more resistive for lower voltages. This behavior shows that when the voltage is lowered, the displacement current in the sheath (capacitive component) decreases faster than the ion current to the electrode (resistive component). Once again the agreement between the two models and the experiments is good. The discrepancy appearing between models and experiment represents in fact only a phase shift less than  $6^\circ$  and is within the error bars of the experimental measurements.

Figure 8 shows the power deposited in the discharge as a function of applied rf voltage for the same conditions.

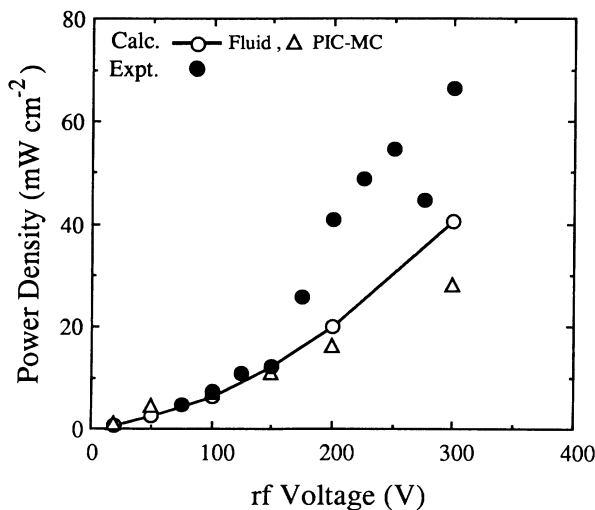


FIG. 8. Power dissipated in a rf discharge in pure argon as a function of applied rf voltage from experiments and fluid and PIC-MC models; same conditions as in Fig. 2.

Experimentally the power is deduced from the measurement of the current, the voltage and the phase shift. As it can be expected from Figs. 6 and 7 the numerical results and the experimental measurements compare well.

The results obtained in this section indicate that (1) although the fluid model does not reproduce perfectly some features such as the spatial distribution of the ionization rate, the predictions of the models are valid in a large range of rf voltages under the conditions of pressure and frequency considered, and (2) both fluid and PIC-MC models can reproduce well the electrical properties of the pure argon discharge deduced from the experiments.

### B. Discharge in contaminated argon

The results presented in this section have been obtained for conditions of pressure, geometry, and frequency identical to those described above (argon pressure 0.11 torr, gap length of 3.3 cm, frequency of 13.56 MHz, and applied rf voltages from 50 to 300 V). Dust particles with concentration of  $10^8 \text{ cm}^{-3}$  and size  $0.1 \mu\text{m}$  have been introduced in the plasma both in the experiments (see Sec. II) and in the models (see Sec. III).

#### 1. Charged-particle densities, electric field, and ionization rate deduced from the models

Figure 9 shows the spatial variations of the electron and ion densities, charge density of dust particles, and electric field at the beginning of the rf cycle for a dusty argon discharge at 200 V. The results have been obtained by the two-electron-group fluid model adapted to account for the presence of dust particles (see Sec. III), with the parameters  $Z_D$  and  $\nu_D$  set to 30 elementary charges and  $3 \times 10^6 \text{ s}^{-1}$ , respectively (as given by the 2D PIC-MC simulation for dust particle concentration and radius of  $10^8 \text{ cm}^{-3}$  and  $0.05 \mu\text{m}$ ). It appears in Fig. 9 that due to the large electron loss frequency on the dust particles the electron density is now much lower than in the case of

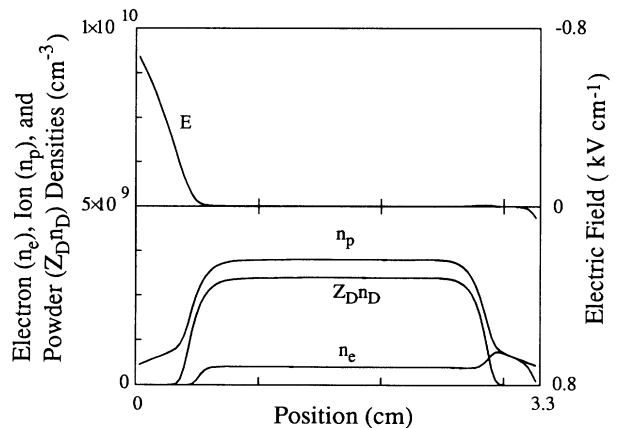


FIG. 9. Spatial variations of the charged particle number densities, charge number density of dust particles, and electric field at the beginning of a rf cycle in argon contaminated with dust particles (0.11 torr, 13.56 MHz, density and size of dust particles  $10^8 \text{ cm}^{-3}$ ,  $0.05 \mu\text{m}$ ) obtained with a fluid model.

pure argon (Fig. 2). The plasma is dominated by positive ions and negatively charged particles and the density of ions and powder is spatially uniform as in the case of a positive column. The important loss of electrons and ions to the particles has been compensated by an increase in the ionization rate in the bulk plasma which has been made possible by an increase in the amplitude of the plasma electric field (11 V/cm, to be compared with 1 V/cm in the case of pure argon).

At this point it is necessary to check that the predictions of the fluid model are coherent with the 2D PIC-MC simulation of Ref. [7]. As described above the fluid model uses as input the number of negative charges of the dust particles,  $Z_D$  and the electron loss frequency  $\nu_D$  given by the simulations of Ref. [7]. We must check that the plasma properties such as electric field and electron to ion density ratio deduced from the fluid model are consistent with those predicted by the 2D PIC-MC simulation. The amplitude of the plasma electric field deduced from the fluid model under the conditions of Fig. 9 is on the order of 11 V/cm (rms value 8 V/cm) and is therefore consistent with the value of the dc electric field (8 V/cm) which is obtained with the model of Ref. [7], for a dust particle radius of  $0.05 \mu\text{m}$ . This is not surprising since the plasma field has to adjust in such a way that the ionization frequency is equal to the electron loss frequency to the dust particles and since, as was shown in Ref. [7], the electron distribution function (EDF) in a dusty plasma under the conditions considered here is close to the EDF in a pure argon plasma for the same value of the electric field (we use in the fluid model the same ionization frequency versus field as in pure argon). The ratio between the electron and ion density in the discharge model (of the order of 7, see Fig. 9) is also coherent with the results obtained with the 2D PIC-MC model (of the order of 10 for the same current density).

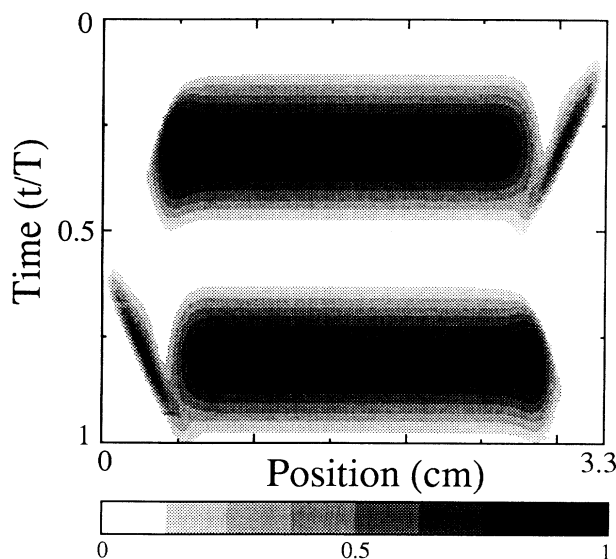


FIG. 10. Space and time variations of the ionization rate over one rf cycle in dusty argon in the conditions of Fig. 9; fluid model, unit =  $6.2 \times 10^{15} \text{ cm}^{-3} \text{ s}^{-1}$ .

The main features of the discharge in the presence of powders as deduced from the fluid model are very similar to those known from models [16,17,27,28] and experiments [28] in electronegative gases. Figure 10 shows the spatial and temporal variations of the ionization rate for a dusty discharge in argon at 200 V. An important change with respect to the case of pure argon displayed in Fig. 5 is that most of the ionization now takes place in the bulk plasma due to the high value of the electric field needed to balance the electron and ion losses in this region (the contribution of the sheath expansion to the total ionization stills exists and appears clearly in Fig. 10). Note also the existence of a local maximum of the ionization rate close to each electrode immediately before the anodic part of the cycle for this electrode. This feature is characteristic of rf discharges in electronegative gases and has been discussed for example in Refs. [17,28].

## 2. Current-voltage characteristics: Comparisons between model and experiments

Figure 11 shows the variation of the total current density as a function of the applied voltage. The results obtained by the fluid model reproduce quite well the current obtained experimentally. As in the case of pure argon, the current density varies quite linearly from a fraction of  $\text{mA cm}^{-2}$  to a few  $\text{mA cm}^{-2}$ . The numerical results are given in Fig. 11 for two values of the electron loss frequency to the dust particles,  $3 \times 10^6 \text{ s}^{-1}$  (corresponding to the 2D PIC-MC calculations of Ref. [7] for a dust particle radius of  $0.05 \mu\text{m}$ ), and  $8 \times 10^6 \text{ s}^{-1}$  (given in Ref. [7] for a dust particle radius of  $0.1 \mu\text{m}$ ). It appears that the calculated current density is not very sensitive to the value of  $\nu_D$  in this range.

Figure 12 shows the variation of the cosine of the current-voltage phase shift for the conditions of Fig. 11. It appears that the pure argon discharge and the dusty

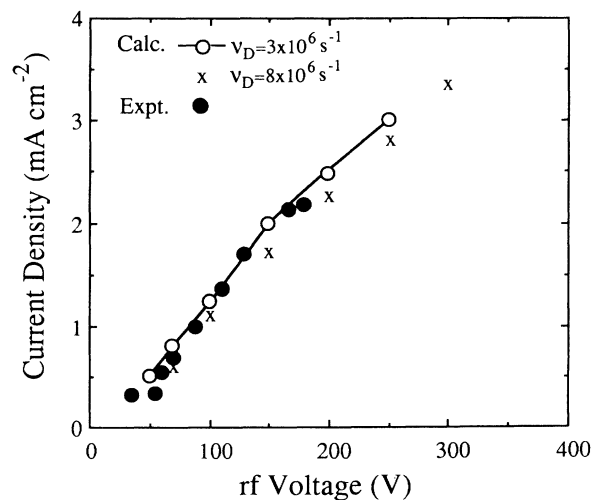


FIG. 11. Current density in a rf discharge in contaminated argon as a function of applied rf voltage from experiments and fluid model (for two values of the electron loss frequency  $\nu_D$  to the dust particles); same conditions as in Fig. 9.



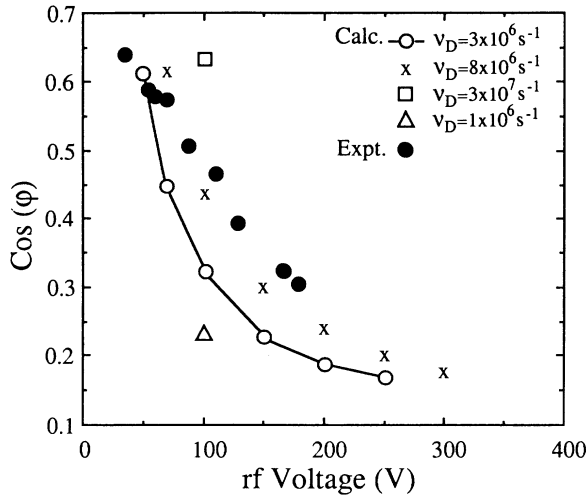


FIG. 12. Cosine of the current-voltage phase shift,  $\cos(\varphi)$ , in a rf discharge in dusty argon as a function of applied rf voltage from experiments and fluid model (for different values of  $\nu_D$ ); same conditions as in Fig. 9.

argon discharge exhibit very different current voltage phase shift (compare Figs. 7 and 12). The measured phase shift is on the order of  $60^\circ$  in the dusty discharge for  $V_{rf}=100$  V instead of  $85^\circ$  in the case of pure argon. The resistive component of the discharge impedance has therefore become much more important in the case of dusty argon. This was expected since the presence of powders in the plasma induces a large increase in the plasma electric field. A similar transition in the discharge impedance had been observed experimentally in a rf discharge in pure silane [8] and had been attributed to the formation of dust particles in the plasma [9]. The phase shift between current and voltage is very sensitive to the presence of powders and this property could be used to help detecting powder formation in a processing plasma. It also appears in Fig. 12 that the results of the discharge model are very sensitive to the value of the electron loss frequency,  $\nu_D$ . The agreement between models and experiments seems to be better for a value of  $\nu_D$  ( $8 \times 10^6 \text{ s}^{-1}$ ) larger than the one ( $3 \times 10^6 \text{ s}^{-1}$ ) deduced from the 2D PIC-MC simulation for the experimental value of the dust particle radius ( $0.05 \mu\text{m}$ ). However, the results shown in Fig. 12 indicate that the model of Ref. [7] provides an estimate of  $\nu_D$  which is in the correct range. We can infer from these results that the model of Ref. [7] gives a realistic description of the electrical properties of dust particles in a nonthermal plasma.

Figure 13 shows the power deposited in the discharge as a function of the applied voltage for the same conditions. As expected from Figs. 11 and 12 the power deposited in the discharge is higher when dust particles are present in the plasma due to the higher resistivity of the discharge in these conditions. The agreement between experimental measurements and numerical results is reasonably good although the predictions of the model are about 30% lower than the measurements for voltages above 150 V. The calculated power dissipation is less

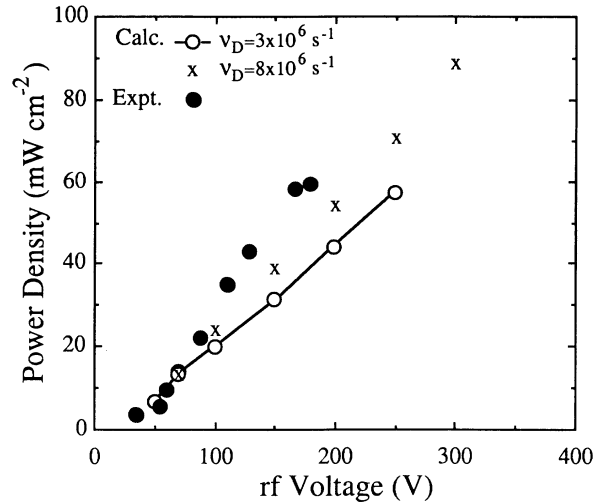


FIG. 13. Power dissipated in a rf discharge in dusty argon as a function of applied rf voltage from experiments and fluid models (for two values of  $\nu_D$ ); same conditions as in Fig. 9.

sensitive to the value of  $\nu_D$  than the calculated current-voltage phase shift shown in Fig. 12.

The increase in the power dissipated in the bulk plasma in the presence of particles has also been confirmed experimentally by observation of the plasma induced optical emission. This was seen to increase dramatically in the presence of particles as shown by the spatially resolved emission of an argon transition ( $750.3 \text{ nm}$ ) (Fig. 14). Note the asymmetry in the emission profile which is due to the small self-bias voltage. These results are consistent with the predictions of the model which show an important increase in the ionization rate in the bulk plasma, in the presence of particles (see Figs. 10 and 4).

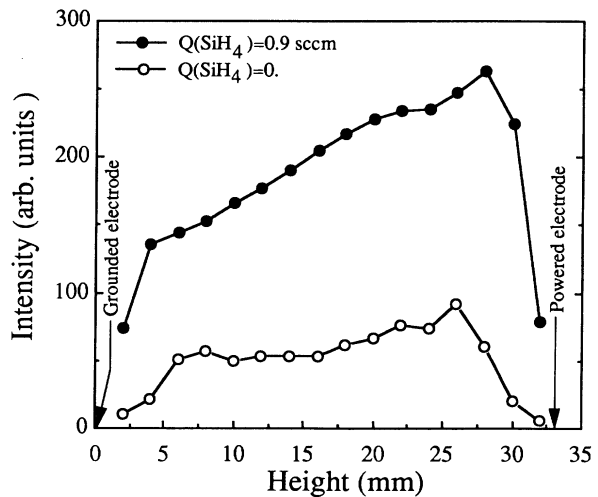


FIG. 14. Spatially resolved optical emission from the argon line  $750.3 \text{ nm}$  with and without dust particles in the plasma [ $Q(\text{Ar})=30 \text{ sccm}$ , amplitude of the rf voltage  $V_{rf}=150 \text{ V}$ ].

## V. CONCLUSIONS

The electrical properties of rf discharges in argon contaminated with dust particles have been analyzed experimentally and numerically and compared with those of similar discharges in pure argon. In the experiments, the dust particles were first created in a silane-argon rf discharge and subsequently trapped in an argon rf discharge. It was therefore possible to study the properties of a dusty plasma where the density and size of the particles stay constant and are known from the experiments.

The discharge models are self-consistent fluid and particle models and can provide the space and time variations of the charged-particle densities, electric field and ionization rates, as well as the current-voltage characteristics of the discharge. These models use as input the number density and size of the dust particles given by the experiments, and the number of negative charges carried by the dust particles and the frequency of electron loss on the dust particles which had been previously determined with a 2D particle-in-cell Monte Carlo simulation of a uniform dc dusty plasma in the conditions of the experiments. This simulation had shown that in these conditions of large dust particle concentration ( $10^8 \text{ cm}^{-3}$ ), the dust particles interact electrostatically (the electron Debye length is larger than the distance between powders) and the classical theory of isolated particles does not apply (the number of negative charges carried by the particles and their floating potential as predicted by this model are much smaller under the experimental conditions than in situations where they can be considered isolated).

The results obtained in the present paper can be summarized as follows.

(1) Comparisons between the results obtained with fluid and PIC-MC models in pure argon show that the under the conditions considered (0.11 torr, 13.56 MHz), the

fluid model reproduces correctly the electrical characteristics of the discharge.

(2) The electrical properties of the discharge (current-voltage characteristics and current-voltage phase shift) predicted by the models in pure and dusty argon are in reasonable agreement with the experiments within the range of voltages considered. This agreement suggests that the 2D PIC-MC model described in the related paper provides a realistic description of the perturbations induced by dust particles in a plasma under the conditions of the experiments. Important qualitative results such as the relatively low number of negative charges (of the order of a few tens) carried by the dust particles and the small floating potential (less than 1 V) predicted by this model in the conditions of the experiments are therefore confirmed.

(3) Experiments and calculations show that the presence of dust particles in the plasma induces an important change in the impedance of the discharge, the discharge being more resistive for large concentrations of particles. This property could be used, in conjunction with other diagnostics, to detect the formation of powders in a processing plasma. The models presented here and in the related paper provides a way to relate the change in the discharge impedance to the concentration and size of the dust particles.

## ACKNOWLEDGMENTS

This work has been supported by CNRS-PIRSEM under Contract No. 89N80/0095, by the CNRS GRECO 57 "Interactions Plasmas Froids-Matériaux" and BRITE-EURAM 690-509224. The Centre de Physique Atomique de Toulouse is "Unité recherche associée no. 277 au CNRS." The Groupe de Recherche sur l'Energétique des Milieux Ionisés is "Unité recherche associée no. 831 au CNRS."

- 
- [1] G. S. Selwyn, J. Singh, and R. S. Bennet, *J. Vac. Sci. Technol. A* **7**, 2758 (1989).
  - [2] M. Anderson, R. Jairath, and J. L. Mock, *J. Appl. Phys.* **67**, 3999 (1990); for other applications of nanoparticle fabrication, see also M. Bawendi, M. L. Steigerwald, and L. E. Brus, *Annu. Phys. Chem.* **41**, 477 (1990); and Y. Wang and N. J. Herron, *J. Phys. Chem.* **95**, 525 (1991).
  - [3] T. J. Sommerer, M. S. Barnes, J. H. Keller, M. J. Mc Caughey, and M. J. Kushner, *Appl. Phys. Lett.* **59**, 638 (1991).
  - [4] M. J. Mc Caughey and M. J. Kushner, *J. Appl. Phys.* **69**, 6952 (1991).
  - [5] M. S. Barnes, J. H. Keller, J. C. Forster, J. A. O'Neill, and D. K. Coultas, *Phys. Rev. Lett.* **68**, 313 (1992).
  - [6] J. E. Daugherty, R. K. Porteous, M. D. Kilgore, and D. B. Graves, *Appl. Phys. Lett.* (to be published).
  - [7] J. P. Boeuf, preceding paper, *Phys. Rev. A* **46**, 7910 (1992).
  - [8] C. Böhm and J. Perrin, *J. Phys. D* **24**, 865 (1991).
  - [9] J. P. Boeuf and Ph. Belenguer, *J. Appl. Phys.* **71**, 4751 (1992).
  - [10] A. Bouchoule, A. Plain, L. Boufendi, J. Ph. Blondeau, and C. Laure, *J. Appl. Phys.* **79**, 1991 (1991).
  - [11] L. Boufendi, A. Plain, J. Ph. Blondeau, A. Bouchoule, C. Laure, and M. Toogood, *Appl. Phys. Lett.* **60**, 169 (1992).
  - [12] G. S. Selwyn, J. P. Mc Killop, and K. L. Haller, *Appl. Phys. Lett.* **57**, 1876 (1990).
  - [13] D. B. Graves and K. F. Jensen, *IEEE Trans. Plasma Sci.* **PS-14**, 78 (1986).
  - [14] D. B. Graves, *J. Appl. Phys.* **62**, 88 (1987).
  - [15] M. S. Barnes, T. J. Cotler, and M. E. Elta, *J. Appl. Phys.* **61**, 81 (1987).
  - [16] J. P. Boeuf, *Phys. Rev. A* **36**, 2782 (1987).
  - [17] J. P. Boeuf and Ph. Belenguer, in *Non Equilibrium Processes in Partially Ionized Gases*, edited by M. Capitelli and J. N. Bardsley, Vol. 220 of *NATO Advanced Science Institute, Series B: Physics* (Plenum, New York, 1990), p. 155.
  - [18] Ph. Belenguer and J. P. Boeuf, *Phys. Rev. A* **41**, 4447 (1990).
  - [19] A. L. Ward, *J. Appl. Phys.* **33**, 2789 (1962).
  - [20] C. K. Birdsall and A. B. Langdon, *Plasma Physics Via Computer Simulation* (McGraw-Hill, New York, 1985).
  - [21] J. P. Boeuf and E. Marode, *J. Phys. D* **15**, 2169 (1982).

- [22] R. W. Boswell and I. J. Morey, *Appl. Phys. Lett.* **52**, 21 (1988).
- [23] M. Surendra and D. B. Graves, *IEEE Trans. Plasma Sci.* **PS-19**, 144 (1991)
- [24] C. K. Birdsall, *IEEE Trans. Plasma Sci.* **PS-19**, 65 (1991).
- [25] P. Ségur and M. C. Bordage, in *Proceedings of the Twenty-Ninth International Conference on PIG*, edited by V. J. Zigman (Studio Plus, Belgrade, 1989); and (private communication).
- [26] A. von Engel, *Ionized Gases* (Oxford University Press, New York, 1965).
- [27] M. Meyyapan and T. R. Govindan, *IEEE Trans. Plasma Sci.* **PS-19**, 122 (1991).
- [28] E. Gogolides, J. P. Nicolai, and H. H. Sawin, *J. Vac. Sci. Technol. A* **7**, 1001 (1989).

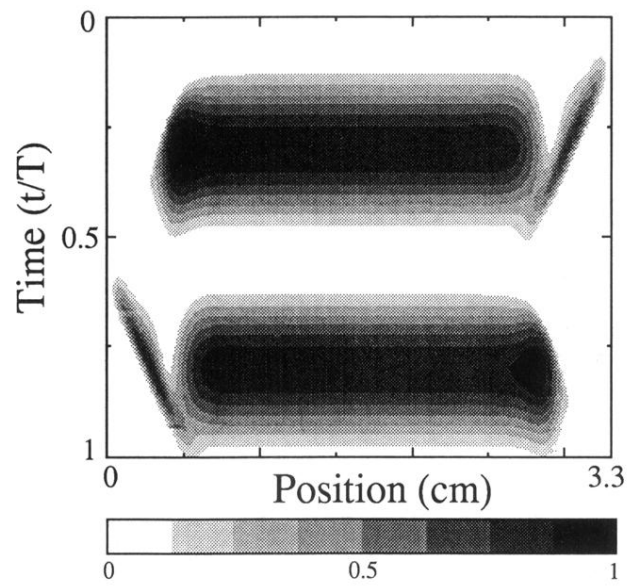


FIG. 10. Space and time variations of the ionization rate over one rf cycle in dusty argon in the conditions of Fig. 9; fluid model, unit =  $6.2 \times 10^{15} \text{ cm}^{-3} \text{ s}^{-1}$ .

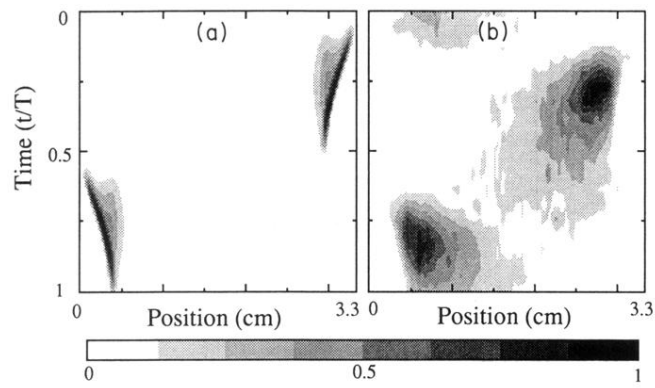


FIG. 4. Space and time variations of the ionization rate over one rf cycle in pure argon in the conditions of Fig. 2; (a) fluid model, unit =  $6.2 \times 10^{15} \text{ cm}^{-3} \text{ s}^{-1}$ ; (b) PIC-MC model, unit =  $1.7 \times 10^{15} \text{ cm}^{-3} \text{ s}^{-1}$ .